Chapter I

Colloidal Nanocrystals: Optical, Catalytic and Magnetic Properties

1.1 Introduction

Colloidal inorganic nanocrystals (NCs) are among the most fertile nanomaterial platform on which the current scientific revolution of nanoscience and nanotechnology is being founded. They are relevant both to the fundamental understanding of the dimensionality-dependent laws of nanosized matter and to the bottom-up development of unprecedented functional materials, devices and processes. At the nanoscale, unique effects, such as the variation of the electronic state density and of magnetic moments, charge redistribution, and/or lattice reconstruction at the material surface, systematically evolve with size and jointly impact on the chemical, magnetic and optoelectronic response of nanostructures, relative to those of their bulk material counterparts. A variety of intriguing solid-state properties coupled with facile post-synthesis processability make NCs a major class of attractive "man-made" materials. Indeed, colloidal NCs serve as unique vehicles to bring the functions of crystals in solution phase. The origin of the size-dependence of optical, electronic, magnetic and catalytic properties in NCs will be described in the following sections.

1.2 The structure of colloidal nanocrystals

Colloidal NCs are composed of an inorganic crystalline core and a surface shell of surfactant or ligand molecules, which coordinate to unsaturated surface atoms (**Fig. 1.1a**). Due to such organic surface capping, NCs can be solubilized in a variety of solvents, embedded in a polymeric matrix, immobilized on substrates, integrated into electrical circuits, or have their surface intentionally modified with biological molecules or with another inorganic material. Because the properties of NCs are influenced both by the inner core and the ligands on its surface, several tools have to be combined to characterize both parts in detail.

Structural-compositional investigation of the inorganic part is carried out mainly by employing low-resolution transmission electron microscope (LR-TEM), high-resolution transmission electron microscope (HR-TEM), electron diffraction (ED), powder X-ray diffraction (XRD) and solid-state Raman spectroscopy. Other more elaborated techniques, such as Mossbauer spectroscopy, the X-ray absorption or fluorescence spectroscopy (XAS/XFS), may generally be used as complementary

tools.^{6,7} For example, in the case of iron oxide neither XRD or Raman spectroscopy allow one to distinguish between the two spinel structures of magnetite (Fe₃O₄) and maghemite (γ-Fe₂O₃), whereas their discrimination can be accomplished by means of Mossbauer or X-Ray based spectroscopies.⁶

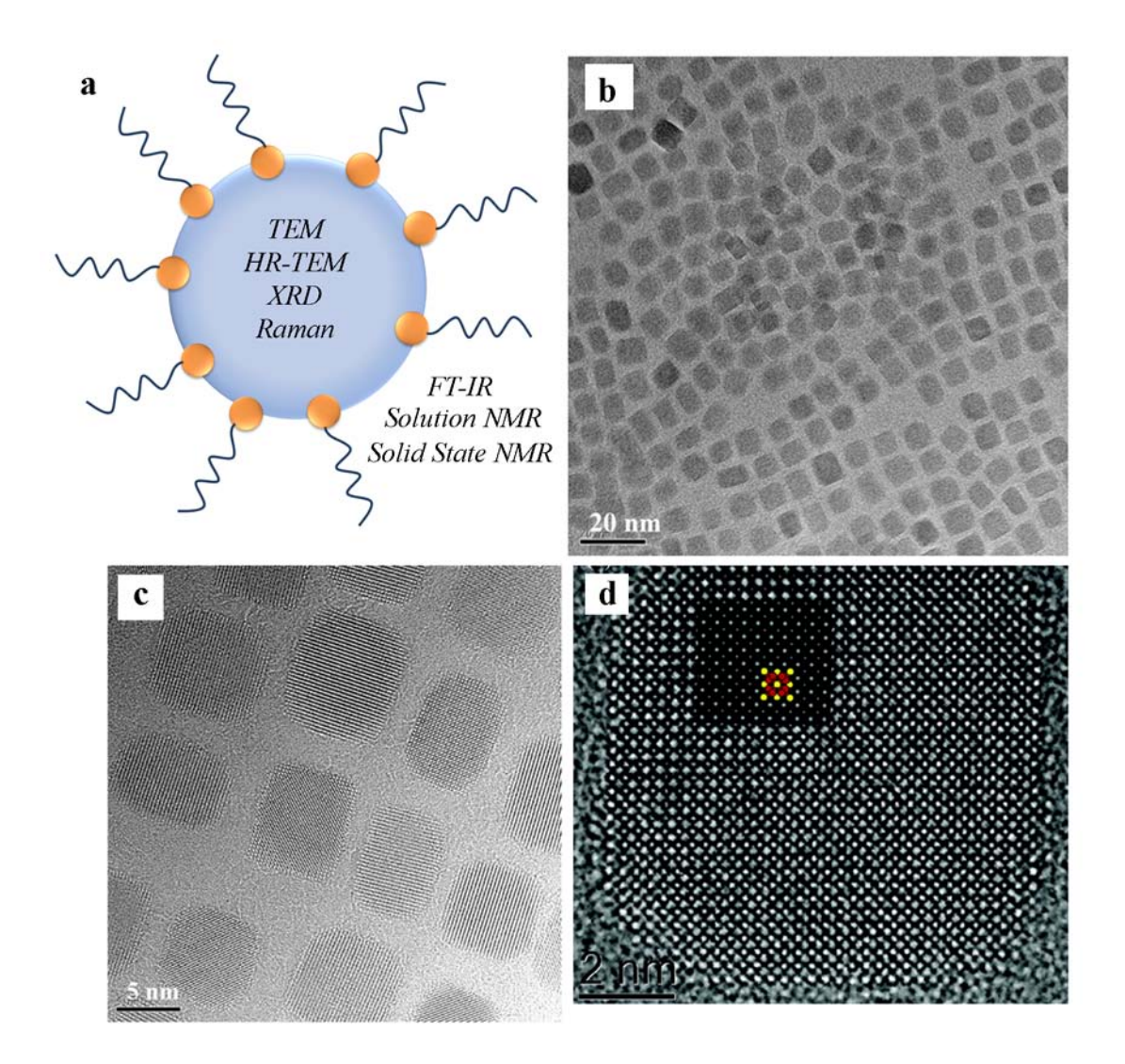


Figure 1.1 (a) A schematic representation of a colloidal NC. (b, c) Representative LR-TEM images at different magnifications of CeO₂ NCs. (d) HRTEM image of an individual CeO₂ NC. A simulated image is superimposed onto the experimental image (yellow = Ce, red = O, respectively). (adapted from ref. 5).

In **Figure 1.1**, LR-TEM (**Figure 1.1b,c**) and HR-TEM (**Figure 1.1d**) images of CeO₂ NCs are shown as examples. LR-TEM images provide an overview of the size and shape of NCs in the sample, while HR-TEM data allows evaluating the crystallinity of individual NCs and analyzing how the atoms are arranged in their lattice.⁵ The presence of point, linear or planar defects, which often represent important details for deducing the NC growth mechanism, can eventually be detected. By measuring the distances and the angles between the visible projected atomic columns by means of fast Fourier transform analysis of the HRTEM image, the crystal polymorph composing the inorganic core of NCs can be identified. A further confirmation of the crystal phase can be given by XRD^{8, 9} or ED (which are based on the Bragg's law), and by the solid-state Raman spectroscopy¹⁰ (which probes the

quantized vibrations, called phonons, across the crystal lattice), which, differently from HR-TEM, describe the sample crystal structure on a statistically meaningful basis.

Common analytical tools for investigating the organic species associated with NCs are fast Fourier Transform Infrared (FTIR) spectroscopy and Nuclear Magnetic Resonance (NMR) spectroscopy.⁴ An IR spectrum represents a fingerprint of the chemical structure of organic surfactants or ligands attached to the NC surface, as it discloses the characteristic vibrations associated with the bonds in the molecules. Although FTIR has frequently demonstrated to be a powerful tool for monitoring the chemical processes that accompany the formation of NCs.¹¹⁻¹⁷ Complementary information can be obtained by conventional solution NMR spectroscopy, which is very sensitive to the chemical environment of atomic species and may allow precise determination of the ligand chemical structure.¹⁸⁻²¹ Its intrinsic limit resides within the scarce capability of distinguishing between organic species in solution and those bound to the NC surface, which can be satisfactorily overcome by using its variant, solid-state NMR spectroscopy.²²⁻²⁴

1.3 General properties of nanocrystals

As previously mentioned, the main parameters influencing the peculiar properties of NCs are their size and shape. An additional important aspect accounting for the exclusivity of NCs is related to the significant fraction of atoms residing on the surface. This justifies great efforts of the scientific community toward developing rational synthetic protocols for finely tuning the NC geometric parameters.^{25, 26} The main synthetic strategies used for controlling the formation of NCs will be presented in Chapter 2. Here, we will examine the main impact of the size, shape and surface of NCs on their optical, catalytic and magnetic properties.

1.3.1 Optical properties

The unique optical properties shown by semiconductor NCs (such as CdSe, CdS, CdTe, InP, InAs, ZnSe, ZnTe) are strictly related to the "quantum confinement effect". The semiconductor reaches the de Broglie wavelength of the associated charge carriers, the motion of the latter becomes restricted to one or more spatial dimensions, giving rise to quantization effects. The so-called "quantum dots" are semiconductor NCs whose electron wavefunctions are confined in three dimensions, while nano-wires and -wells show wavefunction confinement in two and one dimension, respectively. With decreasing the particle size, the energetic structure of the quantum dots changes from a continuous-like one to discrete one. A defining characteristic of the modern view of atoms is that the electronic energy levels are discrete and well separated. In contrast, the electronic energy levels of crystalline solids are diffuse bands of states. The bands of solids are centered about the atomic energy levels of the constituent atoms and arise by the repeated splitting of levels, which occurs as more and more atoms are joined together. In a macroscopic solid this leads to the situation where the energy levels are continuous, since the level spacing is always smaller than the thermal

energy at practically useful temperatures. In nanometer-size crystals, the density of electronic energy levels varies smoothly between the atomic and the bulk limits (**Fig. 1.2a-b**). 31, 36, 37

The size dependence of the density of electronic is seen most clearly in the optical absorption spectra of semiconductor NCs (**Fig. 1.2c**). As a function of increasing size, the centre of a band develops first and the edges last. In semiconductor NCs, where the Fermi level lies between the valence and conduction bands, the edges of the bands dominate the low energy optical and electronic behavior (**Fig 1.2a**). Optical excitations across the gap depend strongly on size. In smaller NCs, the threshold energy for absorption is shifted to higher energy, and the spectra start to develop discrete features.^{36, 38}

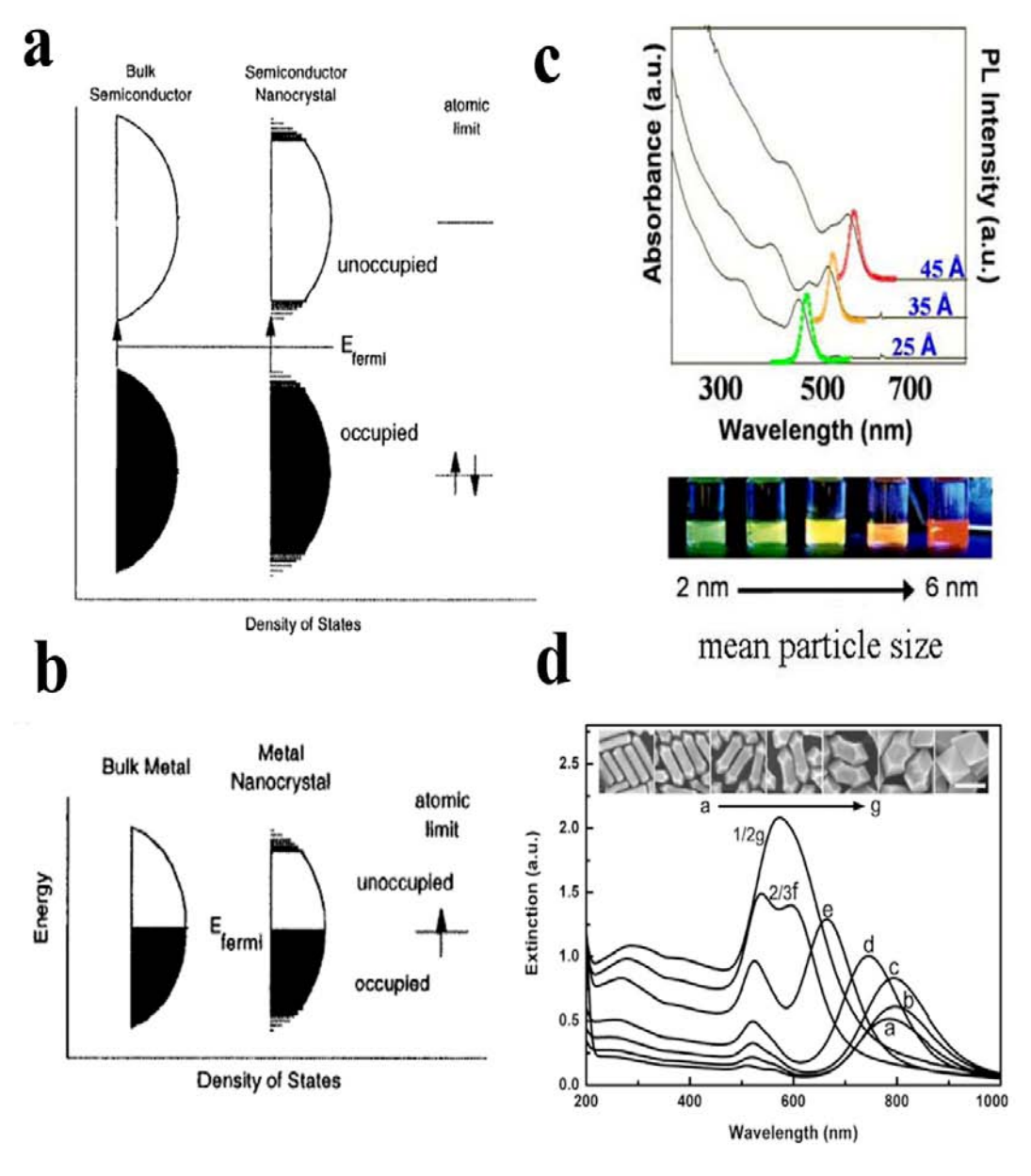


Figure 1.2 Density of states in semiconductor (a) and metal (b) NCs. In both cases, the density of states is discrete at the band edges. (c) Size-dependent absorption and emission spectra of CdSe NCs (top); pictures showing the true colors of solutions of CdSe nanocrystals of varying size (bottom). (d) Size- and shape-dependent absorption spectra of Au NCs (from ref. 49)

The positions of the lowest energy absorption peak (which is usually the most defined) as well as that of the luminescence peak are strictly correlated to the average NC dimensions, while their widths are correlated to the broadness of the size distribution (**Fig. 1.2c**). The peculiar optical size-dependent behavior of semiconductor NCs leads immediately to practical applications. Indeed, they may be thought of as a new class of tunable inorganic dye molecules. Unlike organic dyes, inorganic NCs are robust and resistant to chemical and photochemical alteration, which has allowed them to find use in a wide range of applications, such as in light-emitting diodes, photovoltaics and lasers. ^{31, 39, 40} In biomedical applications, properly functionalized QDs have historically been used as fluorescent probes for ultrasensitive detection of biological molecules, such as DNA or proteins, as well as cancer cells. ⁴¹⁻⁴⁷

Interesting optical properties are shown by metal NCs (Fig. 1.2 b,d). In this case, differently from semiconductors, the Fermi level lies in the centre of a band and consequently the relevant energy level spacing at the band edges is very small (Fig. 1.2b). Thus, at temperature above a few kelvin, the electrical and optical properties more closely resemble those of a continuum, even in NCs with relatively small sizes. Despite quantum confinement does not come into play at any appreciable size, metal NCs show size- and shape-dependent optical absorption spectra. 48-50 This behavior arises from the collective oscillation of conduction electrons under an external electromagnetic field, called surface plasmon resonance (SPR). In coinage metal NCs, the SPR absorption is particularly intense and strongly dependent on the size, while being further modified by the introduction of shape anisotropy (Fig. 1.3d). Whereas spherical NCs show a single SP absorption (dipole resonance), anisotropic-shaped NCs can, in fact, exhibit additional bands, corresponding to quadrupole and higher multipole plasmon resonances. 48-51 This is exemplified in **Figure 1.2d**, where, as the shape evolves anisotropically (cf. images in panels a-g in the inset), two distinct absorption bands appear in the relevant spectra, corresponding to trasverse and longitudinal SPR modes, which are directly related to the mean aspect ratio (that is the ratio of the length to the diameter) of the rod-shaped particles. The characteristic SPR makes metal NCs appealing for nanoscale optics and photonics, as well as for the construction of sensors and biosensors. 52-54 The most exploited properties are probably the dependence of the SPR band position on the NC environment (such as the pH of the solution, or surface adsorption of foreign molecules) and the ability of aggregated metal NCs, and in particular of gold and silver, to increase the optical response of Raman-active molecules in surface-enhanced Raman Scattering Spectroscopy (SERS). 55-60

1.3.2 Catalytic properties

A simple thermodynamic estimation can show that the free energy contribution of surface atoms to the total free energy of a crystal decreases rapidly with an increase in size. It turns out that, due to NCs being characterized by an extremely high surface-to-volume atomic ratio, a high specific surface area is another unique property that distinguishes NCs from their bulk counterparts. As a result, those functionalities of bulk crystals which depend on the surface should be expected to be considerably

enhanced at the nanoscale. Heterogeneous catalysis is one of the most relevant examples in this respect.61-63

The aforementioned changes in the electronic structure brought about by the quantum confinement effect give rise to unusual catalytic properties. The red-ox potential of semiconductor NCs increases as their size decreases, implying that they become more efficient as both reducing and oxidizing species than their bulk counterparts, respectively. Clusters of gold are also found to be catalytically active, while bulk gold is practically unreactive.⁶⁴ In general, metal NCs exhibit a considerable shift of their red-ox potential toward negative values in the nanosized regime, thus serving as efficient electron transfer mediators as well as reductants themselves. 65, 66 Additionally, metal NCs highly dispersed on transition-metal oxide supports are a classical example of a bifunctional catalysts for many oxidation reactions, in which chemisorptive activation of the target molecular substrate on the metal is enhanced by charge transfer between the two inorganic materials, while oxygen atom transfer is promoted by the oxide.67-69

Despite the seeming structural perfection of crystalline nanoparticles, usually the surface of a NC is highly defective. In semiconductor NCs, surface states invariably result in energy levels within the forbidden energy gap. They act as traps for electrons or holes, ultimately leading the degradation of the electrical and optical properties of the material.⁷⁰ In contrast, low-coordination surface atoms, especially in metal and semiconductor oxides are usually beneficial toward catalysis of a variety of chemical reactions.⁷¹⁻⁷⁶ It is well-known that free coordination sites play a major role in transition metal complexes-based catalysis because reactants may bind to these sites and become activated for conversion. Similar considerations are applied to the surfaces of solid catalysts whose surface atoms have generally lower coordination numbers than those situated in the interior of materials. We can easy imagine that unprotected, naked NCs might have a high chemical reactivity. Therefore, another important aspect to take into account in NC-based nanocatalysis is the passivation of the NC surface by organic ligands. Their rational choice has a great importance for the optimization of the catalytic performances of NCs. 75-77 On one side, in the presence of too weak-binding capping ligands, NCs could be, in principle, more available for surface adsorption of reactants. However such NCs could be more susceptible to be destabilized, ripen and/or precipitate under the catalytic reaction conditions, leading to a diminished reactivity over time due to a decrease in active surface exposed to the reactants. On the other side, if surfactants bind to the catalytically active surface sites too strongly and/or the coverage is exceedingly dense, the NCs will be hardly accessible to reactants that need to become activated for conversion.⁷⁵

For a catalytic transformation to occur, certain geometric and energetic requirements must be fulfilled. In this respect, not only the NCs size, which dictates the overall surface area available, is important, but also the shape and the crystal phase, in which the NCs are trapped, do matter. 73, 75, 78 Indeed, differently structured and shaped NCs will offer different sets of exposed crystalline facets as well as a variable distribution of atoms located at corners, edges, steps and point defects, resulting in a substantial energetic heterogeneity and, consequently, influencing the ultimate catalytic performance. 73, 79-82

A particular way by which especially semiconductor oxides, such as TiO₂, ZnO, WO₃, ,CeO₂, can act as heterogeneous catalysts under light stimulation, namely *photocatalysis*, deserves highlight.^{83, 84} The principle of semiconductor photocatalysis is straightforward. Upon absorption of photons with energy larger than the semiconductor band gap, electrons are excited from the valence to the conduction band, creating electron-hole pairs. The photogenerated charge carriers migrates to the surface, where they can initiate a variety of red-ox reactions, which can be exploited for uses as diverse as the degradation of organics, selective conversions of organic products, water splitting for clean and sustainable hydrogen energy production.⁸⁵⁻⁸⁹

1.3.3 Magnetic properties

In this section the magnetic properties of NCs will be demonstrated to be size-dependent properties, like the optical and the catalytic ones. 90-94

Intrinsic magnetism is a property that derives from the arrangement of magnetic dipoles inside a material in absence and/or in presence of an external magnetic field. Depending on the magnetic response observed, magnetic materials can be classified as diamagnetic (DM), paramagnetic (PM), ferromagnetic (FM), ferrimagnetic (FiM) and antiferromagnetic (AFM). A DM material has no magnetic dipole in the absence of external magnetic field, whereas it can exhibit a weak induced magnetization that responds in the opposite direction to an applied field. A material in a paramagnetic (PM) phase is characterized by randomly oriented (or uncoupled) magnetic dipoles, which can be aligned only in the presence of an external magnetic field and along the direction of the layer. This type of material has no coercivity nor remanence, which means that when the external magnetic field is switched off, the internal magnetic dipoles randomize again, no extra energy is required to demagnetize the material and, hence, the initial zero net magnetic moment is spontaneously recovered. Alternatively, the individual magnetic dipoles in a crystal can align parallel one to the other, hence exhibiting an enhanced collective response even in the absence of an external magnetic field. This corresponds to the behavior of FM materials. Bulk metals, such as Fe, Co or Ni as well as their alloys (FePt, FeCo), are FM materials. In contrast, there can be circumstances in which neighboring magnetic dipoles can align antiparallel in the lattice, implying that they will cancel each other (repulsion of magnetic dipoles). This type of magnetic exchange can lead to either AFM materials, in which the magnetic dipoles or interacting spins have the same value and hence the material shows a net zero magnetization, or FiM materials, in which coupled spins possessed different values and, therefore, a net non-zero magnetic dipole different will still hold in the material, even in the absence of an external magnetic field. Magnetite (Fe₃O₄) and maghemite (γ-Fe₂O₃) belong to this class, as Fe atoms with different valence and, hence, with different magnetic moments associated, are co-exist within the same crystal. Examples of AFM materials include some oxides, such as MnO or CoO.

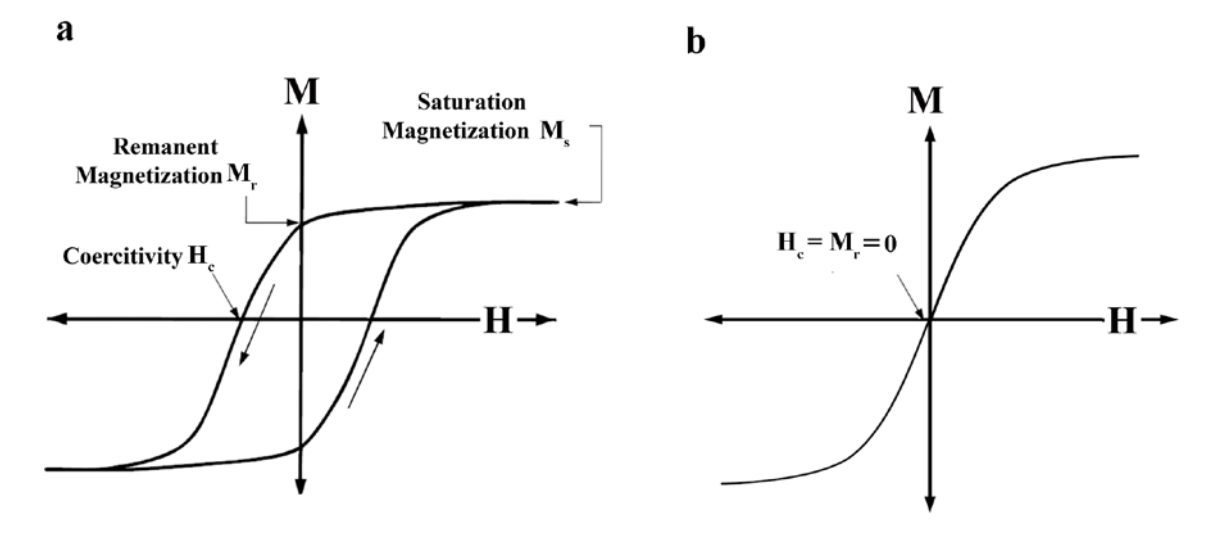


Fig. 1.3 Typical magnetization vs. applied field curve, i.e., hysteresis loop, for a ferro-/ferri-magnetic (a) and a superparamagnetic material (b).

The main parameters that describe the magnetic behavior of FM and FiM NCs can be derived by measuring changes in the magnetization, M, as a function of the strength of an externally applied magnetic field, H. The typical trend, known as hysteresis loop, is displayed in **Figure 1.3**. The hysteresis cycle shows that the application of progressively higher magnetic field makes M of the material accordingly increase up to a maximum value, corresponding to the saturation magnetization, M_S , at which all the dipoles are oriented along the field. The remanent magnetization, M_r , or remanence, is the magnetization value that is measured once the applied magnetic field has been removed (at H=0 in **Fig. 1.3**), while the coercivity, H_c , is the field that has to be applied in the opposite direction for M to recover back to zero.

In general, in a bulk ferro- or ferri-magnetic material, the dipoles are not all parallel to each other; rather there is a distribution of multiple magnetic domains, known as Weiss domains, as depicted in **Figure 1.4a**. The differently aligned magnetic domains are separated from each other by domain walls. Magnetization reversal thus occurs through the nucleation and motion of these walls. **Figure 1.4b** illustrates that, as the NC size decreases down to some critical particle diameter, r_c (ranging from 10 to 100 nm, depending on the typical material parameters), the formation of domain walls becomes energetically unfavourable and the NCs behave as single magnetic domain particles. In single-domain NCs, changes in magnetization can no longer occur through domain wall motion and require the coherent rotation of spins. The energy barrier that has to be overcome for the total magnetization of the system to align in the direction of the applied external magnetic field is called magnetic anisotropy energy:

$$\Delta E_A = K_A V \sin^2 \theta \tag{1.1}$$

where K_A is the magnetic anisotropy constant, V is the particle volume and θ is the angle between the magnetic moment and the "easy axes" of magnetization (that is the preferential crystallographic direction along which the magnetization lies in the single domain system). K_A is a fundamental feature

and can be understood as resulting from different contributions, among which the magnetocrystalline, shape and surface anisotropy. The *magnetocrystalline anisotropy* is an intrinsic property of a material, which derives from spin-orbit coupling within the crystal structure and basically dictates the "easy axis" directions.

Another contribution to the total magnetic anisotropy is that associated with the *shape*, which is obviously unimportant only for spherical crystals. Asymmetrically shaped NCs can be easily magnetized along their longitudinal axis. As an example, when Co NCs are grown with different shapes, it is observed that the coercivity is enhanced for nanorods relative to nanospheres, due to an extra shape anisotropy contribution in the former. ^{95, 96} The *surface anisotropy* is related to the surface effects on the magnetic properties resulting from the lack of translational symmetry at the boundaries of the NCs.

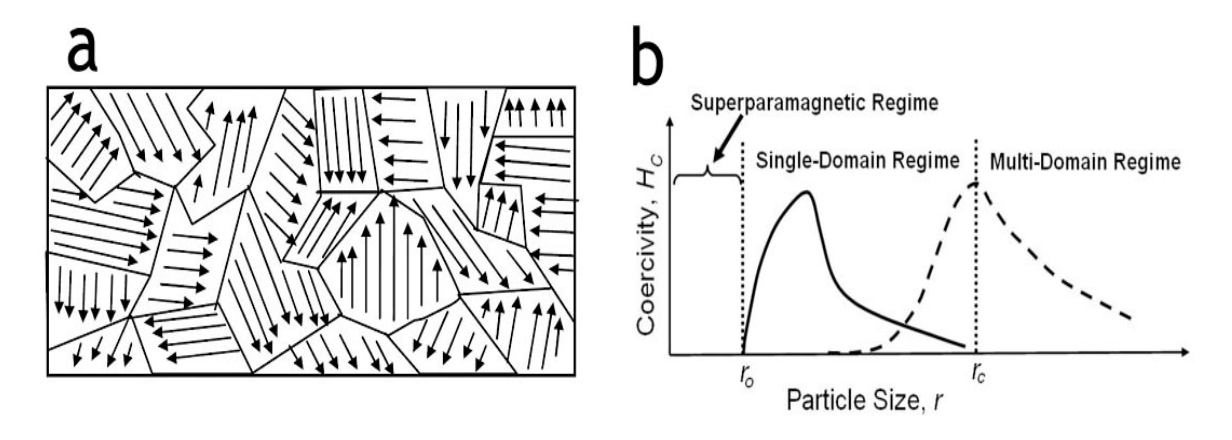


Figure 1.4 (a) Schematic representation of spin distribution across the magnetic domains that compose a bulk material; (b) Size-dependent transition from a multi- to mono-domain configuration in a magnetic material

The lower coordination number of surface atoms and the existence of broken magnetic exchange bonds can lead often to surface spin disorder and frustration (**Fig. 1.5**). Surface effects dominates the magnetic properties in the smallest NCs, since with decreasing the particle size the ratio of surface spins to the total number of spins increases. The presence of a magnetically disordered spin-glass surface layer consisting of canted spins (e.g., in spinel-type oxides) can be responsible for a reduction of the saturation magnetization or an asymmetry in the hysteresis curve (**Fig. 1.5b**). The existence of a magnetic dead layer can be ascribed to different factors, such as a lack of crystallinity at the surface a reduced symmetry depending on a different composition between the core and the surface of simply a poor surface passivation, which could be partially solved by choosing appropriate ligands.

As the particle size decreases below the single domain value and reaches a limiting value (r_0 in **Figure 1.4b**), the anisotropy energy become comparable to the thermal energy (k_BT). In this case the energy barrier can no longer pin the magnetization direction on the time scale of observation and rotation of the magnetization direction occurs due to thermal fluctuations. Such NCs are said to be superparamagnetic. A typical hysteresis curve measured for superparamagnetic NCs is reported in **Figure 1.3b**. The coercitivity of a superparamagnetic particles is zero ($H_C = 0$) because thermal fluctuation prevent the existence of a stable magnetization.

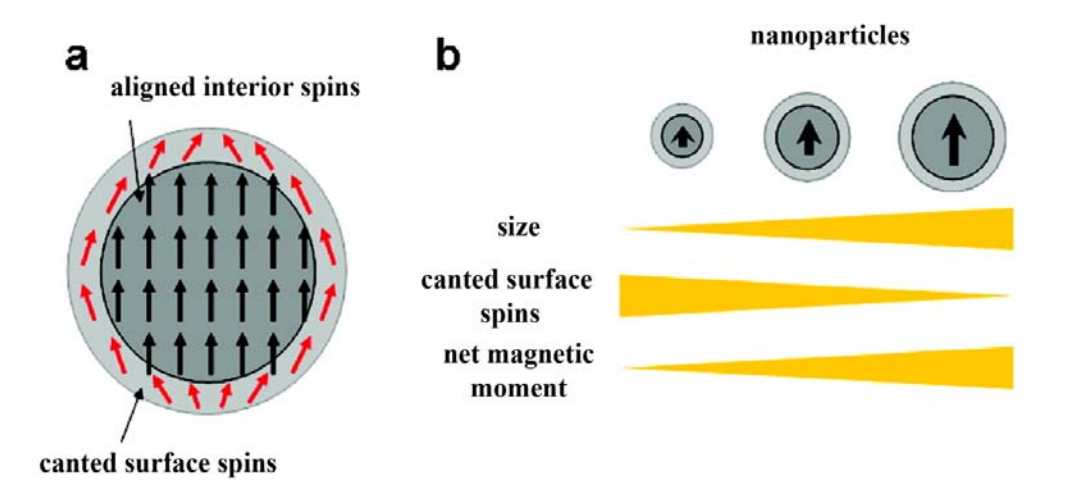


Fig 1.5 Nanocrystal size and surface effects on: (a) canted surface atoms surrounding core magnetic atoms; (b) trend of surface to volume ratio, canted surface spins, net magnetic moment as a function of size (from ref. 98)

Cooling of a superparamagnetic nanoparticle reduces the energy of thermal fluctuations and, at a certain temperature, the free movement of magnetization can be blocked by the anisotropy. The temperature at which the transition from the superparamagnetic to ferromagnetic state takes place is called the blocking temperature (T_B). Information about the blocking temperature can be derived, for example, from the zero-field-cooled (ZFC) and the field-cooled (FC) measuraments (**Fig. 1.6**). In ZFC scans, the sample is cooled without any applied magnetic field to a temperature well below the expected T_B . The system is then warmed up and the magnetization is measured as a function of temperature by applying a small external magnetic field.

As the thermal energy increases, the moments align to the applied field and the magnetization increases. At T_B the magnetization is maximal. Further increase of the temperature above T_B results in a decrease of the magnetization due to the effect of thermal energy causing random fluctuation of the magnetic moments of NCs. In FC scans a sample is cooled in a small external magnetic field, freezing-in a net alignment of the NC moments. The field is then removed, and the magnetization is measured as the sample is slowly warmed up. Thermal energy unpins and randomizes the NC moments, lowering the sample net magnetization. Below T_B the free movement of magnetic moments is "blocked" by the anisotropy. The ZFC/FC curves overlap in the room-temperature-TB range, since in the superparamagnetic regime the thermal energy exceeds the anisotropy barrier and the spins can rapidly change direction (**Fig. 1.6a**). The blocking temperature is a fingerprint of the magnetic behavior of NCs and is tightly dependent on all of their characteristic features, including chemical nature, crystal structure, size, and anisotropy. The relation between T_B and the nanoparticle volume, V, is expressed by the Néel equation: $I^{101, 102}$

$$T_{B=}\frac{K_A}{25K_B}V\tag{1.2}$$

Other frequently observed size effects are the increase in M_S (the sum of more spins leads to a proportionally higher total magnetization) and of the coercitivity Hc with the increase in the particle size (**Fig. 1.4b**). $^{102, 103}$

Superparamagnetic NCs are appealing candidates especially for biomedical applications. ^{94, 103-107} In particular, superparamagnetic iron oxide nanoparticles (SPIOs), showing a high biocompatibility, are widely used both in diagnostics and therapeutics. They are able to enhance the image contrast in magnetic resonance imaging (*MRI*) techniques by modifying the proton relaxation rates in different tissues. ^{94, 105, 106, 108} The NCs induce inhomogeneities in the magnetic field in the surrounding medium, which significantly decrease the transverse relaxation time (T₂) of the protons. The T₂ shortening leads to a signal loss and, in turn, to negatively contrasted images. In MRI applications the main advantage of using NCs in place of traditional gadolinium-based contrast agents resides in the reduction of side-effects in living organisms, thanks to the localized action played by magnetic NCs and to the lower dosage required for obtaining satisfactory, which limits possible toxicity effects. ⁹⁴⁻¹⁰⁴

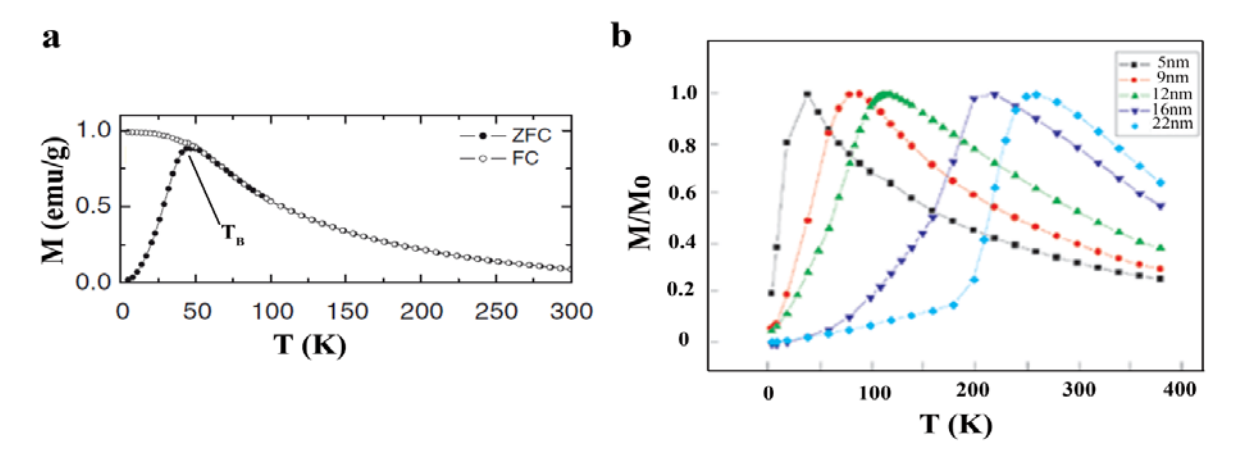


Figure 1.6 (a) Typical magnetization vs. temperature curves measured under zero-field-cooling (ZFC) and field-cooling (FC) conditions. (b) Dependence of the blocking temperature on the size of magnetic nanoparticles (from ref. 101)

Hyperthermia treatments are based on the local heating of tissues for killing cancer cells which are more labile at temperatures above 42°C than their normal counterparts. Magnetic NCs can generate heat under an alternate magnetic field by different mechanisms, such as by a fast physical rotation, the so-called "Brownian rotation". Therefore, their use in hyperthermia has been increasing in the last years. Other applications of biocompatible, appropriately tagged magnetic NCs concern the magnetic separation of specific biological entities, such as DNA, proteins, enzymes, cells, which are present in biological fluids, like blood, with important implications for the early diagnosis of diseases. 94, 107-109 Superparamagnetic NCs are also ideal candidates for drug delivery, which is based on the binding of drugs to the surface of magnetic NCs and their localized release in proximity of a target tissue to which the NCs are transported through the application of an external magnetic field. 94

1.4 Different properties in a single nano-object: hybrid nanocrystals

The advantages arising from the peculiar behavior of nanosized matter can be combined and, hence, further extended by fusing various single-component NCs into a unique multifunctional nano-

object potentially able to perform multiple tasks simultaneously because of the association of material sections with magnetic, optical, catalytic properties. Last-generation breeds of so-called hybrid NCs (HNCs) are structurally elaborated multi-material colloidal nanostructures, consisting of two or more different material domains interconnected through permanent chemical bonding, eventually forming heteroepitaxial interfaces.

The technological horizons that these HNCs can potentially spam are incredibly vast. The grouping of luminescent, magnetic and catalytic sections in individually processable particles—is particularly beneficial to boost those applicative fields, which naturally demand for "smart" platforms able to accomplish multiple actions, such as biomedicine, environmental clean-up, catalysis, sensing. For example, the most promising prototypes of nanoheterostructures comprise a magnetic material section (such as of iron oxide, metal ferrite, FePt) and an optically active material domain (e.g., a semiconductor or a noble metal), which has been used as biological probes for magnetic/optical imaging, sensing, targeted drug delivery, and magnetic separation (**Figure 1.7**). 113-116

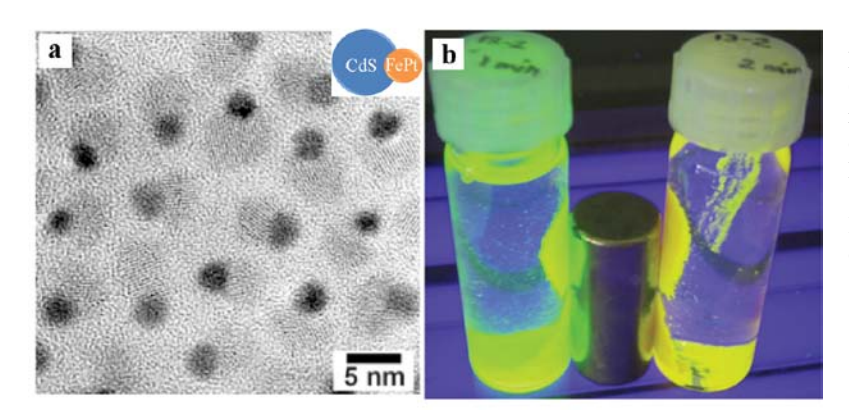


Figure 1.7 (a) TEM image of CdS/FePt heterodimers (from ref. [116]). (b) Photograph of a colloidal dispersion of Fe₃O₃/CdSe heterodimers showing the magnetic and luminescent properties of the composites (from ref. 118)

An additional advantage of HNCs is that they can offer more than one surface platforms available to selective functionalization, which is especially important in biomedicine, catalysis, and sensing. For example Au-Fe₃O₄, Au-FePt, and Ag-Fe₃O₄ heterodimers have been exploited as dual functional probes upon site-selective functionalization with different biomolecules. The processed HNCs have been made simultaneously hydrophilic, fluorescent, responsive to magnetic forces, and capable to bind to specific receptors. ^{117, 118}

The creation of asymmetrically functionalized material sections has been also envisioned as a strategy for promoting the self-assembly of HNCs into functional mesoscopic NC-based "superstructures". 110-113, 119

In HNCs proximity effects can slightly modify the properties of neighboring domains and lead to novel physical-chemical responses. As an example, the growth of Au NC section on CdSe and PbSe NCs has led to photoluminescence quenching while favoring charge separation, which enhances charge transport properties. Similarly, it has been observed that the catalytic performances of oxide NCs, like TiO₂ or ZnO, are improved by depositing noble metal grains their surfaces, which allows metal-enhanced electron transfer to acceptor species. Additionally, the optical properties of noble metal NCs can be slightly changed when bound to other inorganic domains in the form of

HNCs. Au-Fe₃O₄ HNCs, for example, show a red shift of the surface plasmon resonance adsorption band, indicating that the Au section is electron-deficient due to interface communication with iron oxide.¹²³

References

- 1. Alivisatos, A.P. *Endeavour* **1997**, 21, 56-60.
- 2. Rao, C.N.R.; Kulkarni, G.U.; Thomas, P., J.; Edwards, P. P. Chemistry-a European Journal 2002, 8, 29-35.
- 3. Roduner, E. Chem. Soc. Rev. 2006, 35, 583-592.
- 4. Peng, X. Nano Res. 2009, 2, 425-447.
- 5. Kaneko, K.; Inoke, K.; Freitag, B.; Hungria, A. B.; Midgley, P. A.; Hansen, T. W.; Zhang, J.; Ohara, S.; Adschiri, T. *Nano Lett.* **2007**, **7**, 421-425.
- 6. Corrias, A.; Mountjoy, G.; Loche, D.; Puntes, V.; Falqui, A.; Zanella, M.; Parak, W. J.; Casula, M. F. *J. Phys. Chem. C* **2009**, 113, 18667-18675.
- 7. Yuhas, B. D.; Habas, S. E.; Fakra, S. C.; Mokari, T. ACS Nano 2009, 3, 3369-3376.
- 8. Chrosch, J. and Salje, E. K. H. *Ferroelectrics* **1997**, 194, 149
- 9. Guinier, A. "X-Ray Diffraction In Crystals, Imperfect Crystals, and Amorphous Bodies" Courier Dover Publication, New York: 1994
- 10. Gouadec, G.; Colomban, P. J. Raman Spectr. 2007, 38, 598 603.
- 11. Nara, M.; Torii, H.; Tasumi, M. J. Phys. Chem. 1996, 100, 19812-19817.
- 12. Thistlethwaite, P. J.; Gee, M. L.; Wilson, D. Langmuir 1996, 12, 6487 6491.
- 13. Alcock, N. W.; Brown, D. A.; Illson, T. F.; Roe, S. M.; Wallbridge, M. G. H. *J. Chem. Soc. Dalton Trans.* **1991**,1, 873-881.
- Barrow, H.; Brown, D. A.; Alcock, N. W.; Clase, H. J.; Wallbridge, M. G. H. J. Chem. Soc. Dalton Trans. 1994, 2, 195-199.
- 15. Barrow, H.; Brown, D. A.; Alcock, N. W.; Errington, W.; Wallbridge, M. G. H *J. Chem. Soc. Dalton Trans.* **1994**, 3533-3538.
- 16. Fa, K.; Jiang, T.; Nalaskowski, J.; Miller, J. D. Langmuir **2004**, 20, 5311-5321.
- 17. Zhang, Z. H.; Zhong, X. H.; Liu, S. H.; Li, D. F.; Han, M. Y Angew. Chem. Int. Ed. 2005, 44, 3466-3470.
- 18. Fritzinger, B.; Moreels, I.; Lommens, P.; Koole, R.; Hens, Z. Martins, J.C. *J. Am. Chem. Soc.* **2009**, 131, 3024-3032.
- 19. Moreels, I.; Fritzinger, B.; Martins, J.; Hens, Z. J. Am Chem. Soc. 2008, 130, 15081-15086.
- 20. Moreels, I.; Martins, J.C.; Hens, Z. Sensors and Actuators B: Chemical 2007, 126, 283-288.
- 21. Iwan, M.; Jose C.M.; Zeger, H. Chem. Phys. Chem. 2006,7, 1028-1031.
- 22. Tachikawa, T.; Takai, Y.; Tojo, S.; Fujitsuka, M.; Majima, T. Langmuir 2006, 22, 893-896.
- 23. Falaras, P.; Arabatzis, I. M.; Stergiopoulos, T.; Papavassiliou, G.; Karagianni, M. J. Mater. Process. Technol. 2005, 161, 276-281.
- 24. Polito, L.; Colombo, M.; Monti, D.; Melato, S.; Caneva, E.; Prosperi, D. J. Am. Chem. Soc. 2008, 130, 12712-12724.
- 25. Kumar, S; Nann, T. Small 2006, 2, 316-329.
- 26. Lee, S.M.; Cho, S.N.; Cheon, J. Adv. Mater. 2003, 15, 441-444.
- 27. Battaglia, D.; Peng, X.G. Nano Lett. 2002, 2, 1027-1030.
- 28. Ahrenkiel, S. P.; Micic, O. I.; Miedaner, A.; Curtis, C. J.; Nedeljkovic, J. M.; Nozik, A. J. *Nano Lett.* **2003**, 3, 833-837.
- 29. Talapin, D. V.; Rogach, A. L.; Kornowski, A.; Haase, M.; Weller, H. Nano Lett. 2001, 1, 207-211.
- 30. Yu, M.W.; Peng, X. G. Angew. Chem. Int. Ed. 2002, 41, 2368-2371.
- 31. Trindade, T.; O'Brien, P.; Pickett, N.L. Chem. Mater. 2001, 13, 3843-3858.
- 32. El-Sayed, M.A. Acc. Chem. Res. 2004, 37, 326-333.
- 33. Alivisatos, A.P. Science 1996, 271, 933-937.
- 34. Brus, L.E. J. Chem. Phys. 1984,80, 4403-9.
- 35. Bawendi, M.G.; Steigerwald, M.L.; Brus, L. Annual Review Of Physical Chemistry 1990, 41, 477-496.
- 36. Millo, O.; Katz, D.; Steiner, D.; Rothenberg, E.; Mokari, T.; Kazes, M.; Banin, U. *Nanotechnology* **2004**,15, R1-R6.
- 37. Smith, A.M.; Nie, S. Acc. Chem. Res. 2009
- 38. Li, L. S.; Hu, J. T.; Yang, W. D.; Alivisatos, A. P. Nano Lett. 2001, 1, 349-351.
- 39. Pinaud, F.; Michalet, X.; Bentolila, L. A.; Tsay, J. M.; Doose, S.; Li, J. J.; Iyer, G.; Weiss, S. *Biomaterials* **2006**, 27, 1679-1687.
- 40. Wang, S. P.; Mamedova, N.; Kotov, N. A.; Chen, W.; Studer, J. Nano Lett. 2002, 2, 817-822.

- 41. Bruchez, M.; Moronne, M.; Gin, P.; Weiss, S.; Alivisatos, A. P. Science 1998, 281, 2013-2016.
- 42. Chan, W. C.; Nie, S.M. Science 1998, 281, 2016-2018
- 43. Taton, T.A.; Mirkin, C.A.; Letsinger, R.L. Science 2000, 289, 1757-1760.
- Michalet, X.; Pinaud, F.; Lacoste, T. D.; Dahan, M.; Bruchez, M. P.; Alivisatos, A. P.; Weiss, S. Single 44. Molecules 2001, 2, 261-276.
- 45. Wu, X. Y.; Liu, H. J.; Liu, J. Q.; Haley, K. N.; Treadway, J. A.; Larson, J. P.; Ge, N. F.; Peale, F.; Bruchez, M. P. Nat. Biotechnol. 2003, 21, 41-46.
- 46. Gao, X. H.; Cui, Y. Y.; Levenson, R. M.; Chung, L. W. K.; Nie, S. M. Nat. Biotechnol. 2004, 22, 969-
- 47. Bagalkot, V.; Zhang, L.; Levy-Nissenbaum, E.; Jon, S.; Kantoff, P.; Langer, R.; Farokhzad, O. C. Nano Lett. 2007, 7, 3065 - 3070.
- 48. Eustis, S.;.E.-Sayed., M.A. Chem. Soc. Rev. 2006, 35, 209 - 217.
- 49. Xiang, Y.; Wu, X.; Liu, D.; Feng, L.; Zhang, K.; Chu, W.; Zhou, W.; Xie, S. J. Phys. Chem. C 2008, 112, 3203-3208.
- 50. Njoki, P. N.; Lim, I.-I.S; Mott, D.; Park, H.-Y.; Khan, B.; Mishra, S.; Sujakumar, R.; Luo, J.; Zhong, C.-J. J. Phys. Chem. C 2007, 111, 14664 - 14669.
- 51. Ni, W.; Kou, X.; Yang, Z.; Wang, J. ACS Nano 2008, 2, 677-686.
- Hutter, E.; Fendler, J. H. Adv. Mat. 2004, 16, 1685-1706. 52.
- Jain, P. K.; Huang, X.; El-Sayed, I. H.; El-Sayed, M. A. Acc. Chem. Res. 2008. 41, 1578-1586. 53.
- 54. Tao, A.; Sinsermsuksakul, P.; Yang, P. Nat. Nanotechnol. 2007, 2, 435 - 440.
- 55. Zhang, D.-F.; Niu, L.-Y.; Jiang, L.; Yin, P.-G.; Sun, L.-D.; Zhang, H.; Zhang, R.; Guo, L.; Yan, C.-H. J. Phys. Chem. C 2008, 112, 16011-16016.
- 56. Doering, W. E.; Piotti, M.E.; Natan, M. J.; Freeman, R. G. Adv. Mater. 2007, 19, 3100-3108.
- 57. Shanmukh, S.; Jones, L.; Driskell, J.; Zhao, Y.; Dluhy, R.; Tripp, R. A. Nano Lett. 2006, 6, 2630-2636.
- Doering, W.E.; Nie, S.M. J. Phys. Chem. B 2002, 106, 311-317. 58.
- 59. Qian, X.; Li, J.; Nie, S. J. Am. Chem. Soc. 2009, 131, 7540-7541.
- 60. Cao, Y.W.C.; Jin, R.C.; Mirkin, C.A. Science 2002, 297, 1536-1540.
- 61. Samorjai G.A.; Park, J.Y. Top. Catal. 2008, 49, 126-135.
- 62. Somorjai, G.A.; Frei, H.; Park, J.Y. J. Am. Chem. Soc. 2009, 131, 16589-16605.
- 63. Zhou, X.; Xu, W.; Liu, G.; Panda, D.; Chen, P. J. Am. Chem. Soc. 2009, 132, 138-146.
- 64. Rao, C. N. R.; Vijayakrishnan, V.; Kumar, A.; Menno, W. J. P. Angew. Chem. Int. Ed. 1992, 31, 1062-1064.
- 65. Mulvaney, P.; Giersig, M.; Henglein, A. J. Phys. Chem. 1993, 97, 7061-7064.
- Henglein, A. Chem. Rev. 1989, 89, 1861-1873. 66.
- 67. Guzman, J.; Gates, B. C. J. Am. Chem. Soc 2004, 126, 2672-2673.
- 68. Awazu, K.; Fujimaki, M.; Rockstuhl, C.; Tominaga, J.; Murakami, H.; Ohki, Y.; Yoshida, N.; Watanabe, T., A J. Am. Chem. Soc. 2008, 130, 1676-168.
- 69. Harding, C.; Habibpour, V.; Kunz, S.; Farnbacher, A.; Heiz, U.; Yoon, B.; Landman, U. J. Am. Chem. Soc. 2009, 131, 538-548.
- 70. Myung, N.; Bae, Y.; Bard, A. J. Nano Lett. 2003, 3, 747-749.
- 71. Li, Y.; Zhang, J. Z. Laser & Photonics Rev. 2009.
- 72. Wang, C.; Yin, H.; Chan, R.; Peng, S.; Dai, S.; Sun, S. Chem. Mater. 2009, 21, 433-435.
- 73. Lee, I.; Delbecq, F.; Morales, R.; Albiter, M. A.; Zaera, F. Nat. Mater. 2009, 8, 132.
- 74. Enthaler, S.; Junge K.; Beller, M. Angew. Chem. Internat. Ed. 2008, 47, 3317-3321.
- 75. Stowell, C.A.; Korgel, B. A. Nano Lett. 2005, 5, 1203-1207.
- 76. Li, S.-C.; Diebold, U. J. Am. Chem. Soc. 2009, 132, 64-66.
- 77. Li, Y.; El-Sayed, M. A. J. Phys. Chem. B 2001, 105, 8938-8943.
- 78. Narayanan, R. El-Sayed, M.A. Nano Lett. 2004, 4, 1343-1348.
- 79. Yang, H. G.; Sun, C. H.; Qiao, S. Z.; Zou, J.; Liu, G.; Smith, S. C.; Cheng, H. M.; Lu, G. Q. Nature 2008,
- 80. Li, W.-K.; Gong, X.-Q.; Lu, G.; Selloni, A. J. Phys. Chem. C, 2008, 112, 6594-6596.
- 81. McGill, P.R.; Idriss, H. Langmuir 2008, 24, 97-104.
- 82. Park, J. B.; Graciani, J.; Evans, J.; Stacchiola, D.; Senanayake, S. D.; Barrio, L.; Liu, P.; Sanz, J. F.; Hrbek, J.; Rodriguez, J.A. J. Am. Chem. Soc. 2009, 132, 356-363.
- 83. Fujishima, A.; Zhang, X. Compt. Rendus Chem. 2006, 9, 750-760.
- Fujishima, A.; Rao, T.N.; Tryk, D. A. J. Photochem. Photobiol. C: Photochem. Rev. 2000, 1, 1-21. 84.
- 85. Fujishimaa, A.; Zhanga, X.; Tryk, D. A. Int. J. Hydrogen Energy 2007, 32, 2664-2672
- 86. Canela, M. C.; Alberici, R. M.; Sofia, R. C. R.; Erberlin, M. N.; Jardim, W. F. Environ. Sci. Technol. **1999**, 33, 2788-2792.
- 87. Palmisano, G.; Augugliaro, V.; Pagliaro, M; Palmisano, L. Chem. Commun. 2007, 33, 3425 - 3437.
- 88. Youngblood, W. J.; Lee, S.-H. A.; Maeda, K.; Mallouk, T. E. Acc. Chem. Res. 2009, 42, 1966-1973.
- 89. Chen, X. Chin. J. Catal. 2009, 30, 839-851.

- 90. Leslie-Pelecky, D.L.; Rieke, R.D. Chem. Mater. 1996, 8, 1770-1783.
- 91. Xavier, B.; Labarta, A. J. Phys. D: Appl. Phys. 2002, 35, R15.
- 92. Frey, N. A.; Peng, S.; Cheng, K.; Sun, S. Chem. Soc. Rev. 2009, 38, 2532-2542.
- 93. Shivang, R.D.; Xiaohu, G. Wiley Interdiscipl. Rev.: Nanomed. Nanobiotechnol. 2009, 1, 583-609.
- 94. Pankhurst, Q. A.; Connolly, J.; Jones, S. K.; Dobson, J. J. Phys. D: App. Phys. 2003, 36, R167-R181.
- 95. Puntes, V.F.; Krishnan, K.; Alivisatos, A. P. *Top. Catal.* **2002**, 19, 145-148.
- 96. Dumestre, F.; Chaudret, B.; Amiens, C.; Respaud, M.; Fejes, P.; Renaud, P.; Zurcher, P. *Angew. Chem. Int. Ed.* **2003**, 42, 5213-5216.
- 97. Morales, M.P.; Veintemillas Verdaguer, S.; Montero, M.I.; Serna, C.J.; Roig, A; Casas, L.; Martinez, B.; Sandiumenge, F. *Chem. Mater.* **1999**, 11, 3058-3064.
- 98. Cheon, J.; Lee, J. H. Acc. Chem. Res. 2008, 41, 1630-1640.
- 99. Tan, Y.; Zhuang, Z.; Peng, Q.; Li, Y. Chem. Mater. 2008, 20, 5029-5034.
- 100. Daou, T. J.; Grene, X.; Che, J. M.; Pourroy, G.; Buathong, S.; Derory, A.; Ulhaq-Bouillet, C.; Donnio, B.; Guillon, D.; Begin-Colin, S. *Chem. Mater.* **2008**, 20, 5869-5875.
- Park, J.; Ann, K.; Hwang, Y.; Park, J.-G.; Noh, H.-J.; Kim, J.-Y.; Park, J.-H.; Hwang, N.-M.; Hyeon, T. Nat. Mater. 2004, 3, 891-895.
- 102. Sun, S. H.; Zeng, H.; Robinson, D. B.; Raoux, S.; Rice, P. M.; Wang, S. X.; Li, G. X. *J. Am. Chem. Soc.* **2004**, 126, 273-279.
- 103. Lu, A.-H.; Salabas, E. L.; Schüth, F. Angew. Chem. Int. Ed. 2007, 46, 1222-1244.
- 104. Jeong, U.; Teng, X. W.; Wang, Y.; Yang, H.; Xia, Y. N. Adv. Mater. 2007, 19, 33-60.
- 105. Bin Na, H.; Song, I. C.; Hyeon, T. Adv. Mater. 2009, 21, 2133-2148.
- 106. Jun, Y.-w.; Huh, Y.-M.; Choi, J.-s.; Lee, J.-H.; Song, H.-T.; Kim, S.-j.; Yoon, S.; Kim, K.-S.; Shin, J.-S.; Suh, J.-S.; Cheon, J. *J. Am. Chem. Soc.* **2005**, **127**, 5732-5733.
- Fu, A.; Hu, W.; Xu, L.; Wilson, R. J.; Yu, H.; Osterfeld, S.J.; Gambhir, S.S.; Wang, S. X. Angew. Chem. Int. Ed. 2009, 48, 1620-1624.
- 108. Thierry, B.; Al-Ejeh, F.; Brown, M. P.; Majewski, P.; Griesser, H. J. Adv. Mater. 2009, 21, 541-545.
- 109. McCloskey, K.E.; Chalmers, J. J.; Zborowski, M. Anal. Chem. 2003, 75, 6868-6874.
- 110. Cozzoli, P.D.; Pellegrino, T.; Manna, L. Chem. Soc. Rev. 2006, 35, 1195-1208.
- 111. Buonsanti, R.; Casavola, M.; Caputo, G.; Cozzoli, P. D. Recent. Pat. Nanotechnol. 2007, 1, 224-232.
- 112. Casavola, M.; Buonsanti, R.; Caputo, G.; Cozzoli, P. D. Eur. J. Inorg. Chem. 2008, 6, 837-854.
- 113. Wang, C.; Xu, C.; Zeng, H.; Sun, S. Adv. Mater. 2009, 21, 3045-3052.
- 114. Quarta, A.; DiCorato, R.; Manna, L.; Ragusa, A.; Pellegrino, T. *IEEE Transaction on Nanobioscience* **2007**, 6, 298-308.
- 115. Gao, J.; Gao, B.Z.Y.; Pan, Y.; Zhang, X.; Xu, B. J. Am. Chem. Soc. 2007, 129, 11928 11935.
- 116. Ang, C. Y.; Giam, L.; Chan, Z. M.; W. H. Lin, A.; Gu, H.; Devlin, E.; Papaefthymiou, G.; Selvan, S. T.; Ying, J. Y. *Adv. Mater.* **2009**, 21, 869-873.
- 117. Gu, H. W.; Yang, Z. M.; Gao, J. H.; Chang, C. K.; Xu, B. J. Am. Chem. Soc. 2005, 127, 34-35.
- 118. Xu, C.; Xie, J.; Ho, D.; Wang, C.; Kohler, N.; Walsh, E.G.; Morgan, J. R.; Chin, Y. E.; Sun, S. *Angew. Chem. Int. Ed.* **2008**, 47, 173-176.
- 119. Salant, A.; Amitay-Sadovky, E.; Banin, U. J. Am. Chem. Soc 2006, 128, 10006-10007.
- 120. Costi, R.; Cohen, G.; Salant, A.; Rabani, E.; Banin, U. Nano Lett. 2009, 9, 2031-2039.
- 121. Elmalem, E.; Saunders, A.; Costi, R.; Salant, A.; Banin, U. Adv. Mater. 2008, 20, 4312-4317.
- 122. Kamat, P.V.; Flumiani, M.; Dawson, A. Colloid Surf. A-Physicochem. Eng. Asp. 2002, 202, 269-279.
- 123. Yu, H.; Chen, M.; Rice, P. M.; Wang, S. X.; White, R. L.; Sun, S. H. Nano Lett. 2005, 5, 379-382.